

Advances in Oscillating Water Column Air Turbine Development

W.K. Tease, J. Lees and A. Hall

Wavegen, 13^a Harbour Road, Inverness, IV1 1SY, United Kingdom
E-mail: ken.tease@wavegen.com

Abstract

This paper describes the methods developed by Wavegen during the design and development phase of its air turbine suitable for installation into active renewable energy breakwater schemes. The main areas of focus are related to design optimisation, product standardisation and refining manufacture methods to enable development of a commercial product.

Different types of parametric frequency and time domain based models were developed to predict the systems':

- Power performance
- Structural component performance
- Acoustic performance

Numerical routines and semi empirical relationships were used to generate the characteristic curves for the power take off system. Site generated experimental data was used for validation purposes.

Due to the bespoke nature of the systems involved Finite Element Analysis (FEA) was used to stress critical components. This information was fed into fatigue analysis routines for component life estimation.

These methods enabled the maximisation of turbine performance, minimisation of construction costs, while ensuring the acoustic signature of the device adhered to international standards under the particular project design constraints imposed. The final product is safe to operate, reliable and easily maintained.

Keywords: Acoustics, Fatigue, Manufacture, Oscillating Water Column, System Optimisation, Wells Turbines

Nomenclature

D	= Applied system damping, (Ns/m ⁵) = $\Delta P/Q$
F	= Force, (N)
N	= Number of cycles
R	= Rotor radius, (m)
S	= Stress, (N/m ²)
SWL	= Sound power level, (dB(A))
T	= Torque, (Nm)
U	= Number of revolutions
ΔP	= Pressure drop, (Pa)
P^*	= Non-dimensional pressure

$$P^* = \frac{\Delta P}{\rho \omega^2 R_t^2}$$

Q	= Flow rate, (m ³ /s)
T*	= Non-dimensional torque

$$T^* = \frac{T}{\rho \omega^2 R_t^5}$$

Phi	= Flow coefficient
ρ	= Air density, (kg/m ³)
ω	= Rotational speed, (Rad/s)

Subscripts

a	= Axial
A	= Alternating
eq	= Equivalent
m	= Miscellaneous
M	= Mean
T	= Tip
u	= Ultimate

© Proceedings of the 7th European Wave and Tidal Energy Conference, Porto, Portugal, 2007

Introduction

This paper describes the methods developed by Wavegen during the design and development phase of its air turbines suitable for installation into active renewable energy breakwater schemes, like the one being built in Mutriku, Northern Spain, ref. Fig.1.



Figure 1: Mutriku Active Breakwater

The breakwater water is located in 7m of water MWL and is NNE facing. The majority of the structure is of a conventional rubble mound construction and has a crescent shape with an overall length off 600m. The active zone

where the oscillating water columns (OWC) are positioned are made from reinforced concrete and are of a novel modular construction. This section covers a central 100m section of the structure and 16 off OWC chambers are housed within. Each chamber has a span and depth of 5.5m x 3.1m respectively. A machine room is located on the top

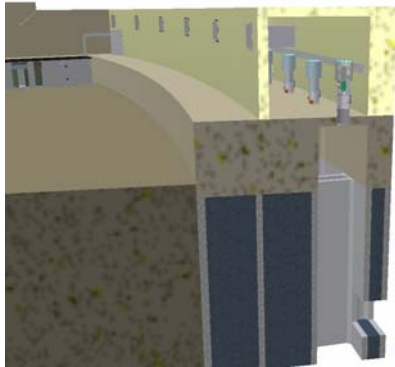


Figure 3: Mutriku Turbine Hall

of the breakwater to house the turbines. The total installed capacity for the system is 296 kW, ref. Fig.2.

To enable Wavegen to deliver with confidence a product which has engineering reliability built in and for a price which the market can sustain; we have drawn on the combined experiences gained through 6 years of testing and operation at the LIMPET test facility, (ref. Fig.3) and VSH's engineering excellence, developed in the hydro business over the last 140 years.



Figure 2: LIMPET Test Facility

Product Development

The main areas of development focus related to design optimisation, product standardisation and refinement of manufacturing methods.

To enable design optimisation to function effectively within typical project time frames, different types of parametric frequency and time domain based models were developed. These are able to predict the systems:

- Power performance
- Structural component performance
- Acoustic performance

Due to the bespoke nature of the systems involved Finite Element Analysis (FEA) was used to stress critical

components. This information was fed into fatigue analysis routines for component life estimation.

These methods enabled the maximisation of turbine performance, minimisation of construction costs, while ensuring the acoustic signature of the device adheres to standards under the particular project design constraints imposed.

Wavegen introduced product standardisation, ref. Fig.4, to help focus the development effort and limit the work required to deliver a complete project with all the necessary supporting documentation. It is important to get this support structure correct for effective product development and project delivery. Wavegen is certified to ISO 9001 design, manufacturing and safety standards. The installed capacity of the product range is 18.5 - 250 kW.



Figure 4: Wavegens Product Range

The final product is safe to operate, reliable and easily maintained.

Project Constraints

Several project constraints were imposed, of which the most important were acoustic emission restrictions, spatial/layout limitations and the incident wave resource.

Incident Wave Resource

A wave resource assessment for the site was carried out by HIDTMA. Using a combination of data from an offshore waverider buoy in deep water at Bilbao-Vizcaya (punto WANA 1068075) and ray tracing methods a series of sea states at the collector location were synthesized, ref. Fig.5.

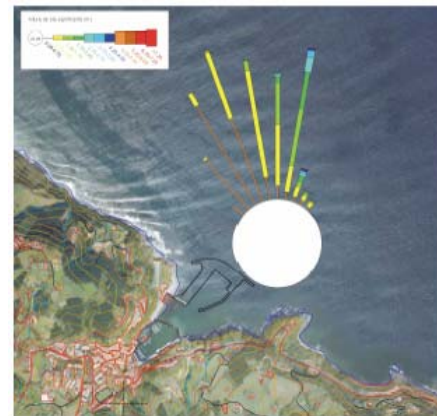


Figure 5: Incident Wave Power Rose

A selection was then made to represent the variation throughout the year of the incident wave power at the site,

ref. Fig.6. An annual average power of 7.14 kW/m was estimated for the location.

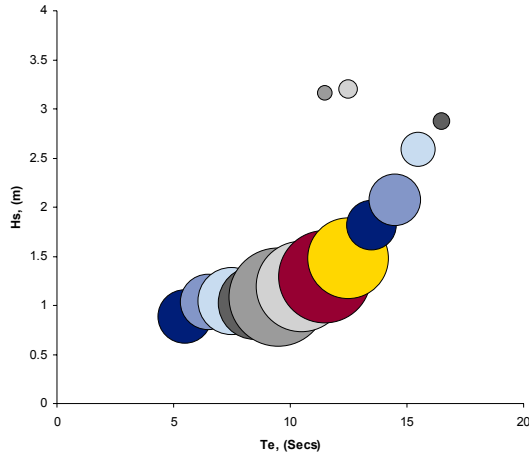


Figure 6: Site Specific Incident Sea States

Wavetank experiments were carried out on the breakwater OWC collector geometry under different sea states and applied damping levels to quantify how the pneumatic power captured varied, ref. Fig.7.

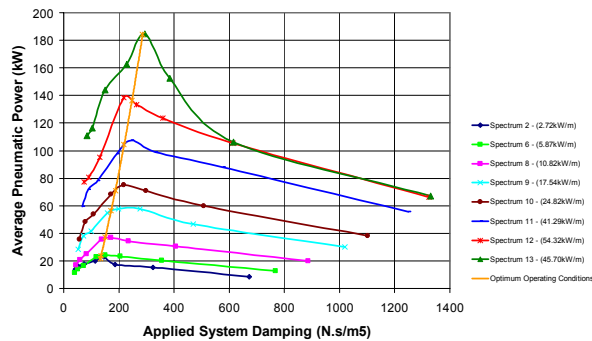


Figure 7: OWC Collector Power Capture Curves

The incident wave resource data and the OWC collector power transfer information was then used as input data for the numerical models.

1 System Power Performance

Various frequency and time domain parametric models of the system have been developed.

The frequency domain models (based on Falcão et al Stochastic approach⁽¹⁻⁴⁾) are used for top level system optimisation.

This enables sizing of the turbine, duct work, generator, inverter etc. and performance predictions given with different control laws imposed. All the basic components are included and their relative importance to the system ascertained for a given OWC collector geometry when subjected to different incident wave energy conditions.

The characteristic curves for the power take off system could be derived from several sources, varying in degrees of detail and hence complexity:

- (1) Analytical parametric system models which are composed of the turbine prime mover, ducting work and valving effects⁽⁵⁾. The simplest being an actuator disk model^(6,7) and most complex being a radial equilibrium strip model^(8,9) with corrections made for the effects of blade interference, Reynolds number and compressibility effects.
- (2) Alternatively results generated from Computational Fluid Dynamic part models of the system under steady state conditions can be used, the details of which are outlined in, ref. (10).
- (3) A semi-empirical database also exists which is based on laboratory and site generated experimental data sets.

Figs. 8 and 9 show correlation between experimental site generated data and numerical results for Wavgens MKIV turbine. Good correlation is achieved in the prestall region, but further research is required for improving the accuracy after stall. Fortunately the turbine does not operate in this region significantly provided the system is properly designed and controlled.

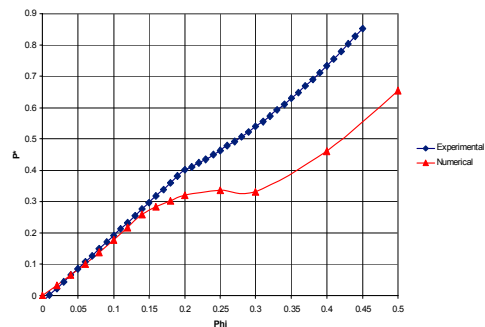


Figure 8: P* vs Phi Experimental/Numerical Correlation for a Biplane Wells Turbine

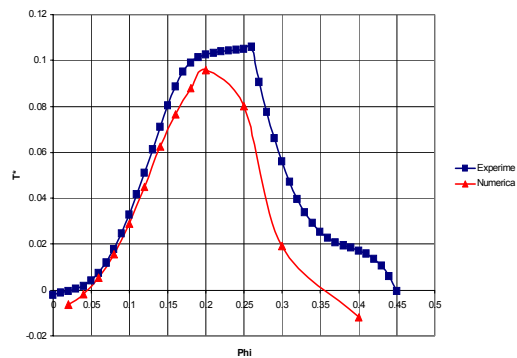


Figure 9: T* vs Phi Experimental/Numerical Correlation for a Biplane Wells Turbine

Figs. 10 and 11 show some sample numerical results of P* and T* vs Phi for a monoplane Wells turbine of different rotor solidities.

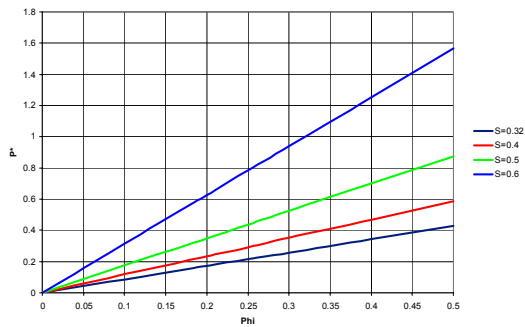


Figure 10: Turbine Non-Dimensional Pressure vs Flow Coefficient for Different Rotor Solidities

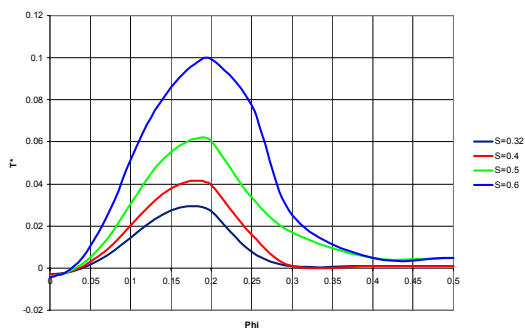


Figure 11: Turbine Non-Dimensional Power vs Flow Coefficient for Different Rotor Solidities

These non-dimensional curves were then used to size the machine and determine operating speed ranges under different turbine configurations/types, control regimes and incident sea states. When optimising it is desirable to aim to satisfy the following requirements:

Key Turbine Design Optimisation Criteria

- High Net Average Cycle Efficiency
- Wide Operational Bandwidth
- High Power Density
- Matching of Turbine Damping & System Damping
- Minimisation of fixed and variable losses
- Low Cost
- Simple Accurate Construction Methods
- Low Maintenance
- Easy Installation
- Reliable
- Low Acoustic Signature
- Space Constraints

These conditions are a mix of both hard and software engineering constraints and depending on the constraints imposed by a specific project, compromises have to be sought when searching for practical solutions. The design of the system must not be too site specific and must be flexible enough so it can be modified to fit into a particular

product range. Product standardisation minimises development and manufacturing costs.

For this particular analysis the diameter of the machine and hub to tip ratio was fixed at 750mm and 0.43 respectively.

Figures 12 and 13 are sample solutions of monoplane and biplane turbine options for the Mutriku project. The effect of rotor solidity, operating speed on the system damping and how this affects the annual average power generated can be clearly seen. The effect on the annual effective operating flow coefficient can also be seen, ref. Fig.14. This indicates how close to stall a particular turbine design is.

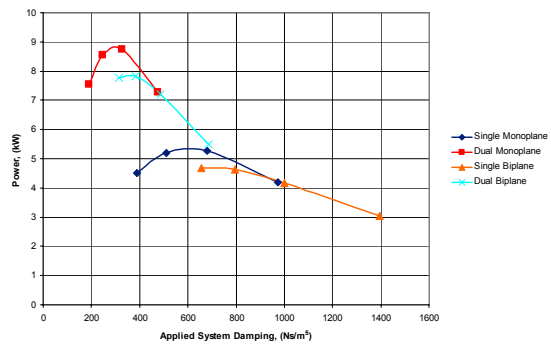


Figure 12: Annual Average Power Generated vs Applied System Damping

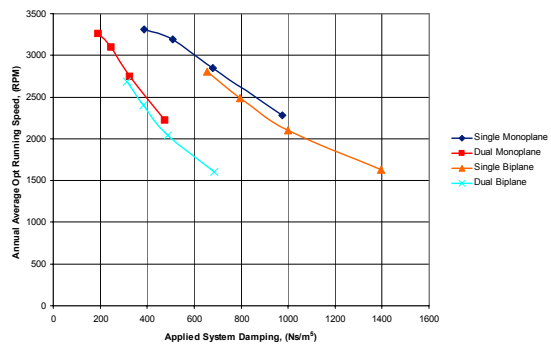


Figure 13: Annual Average Optimum Operating Speed vs Applied System Damping

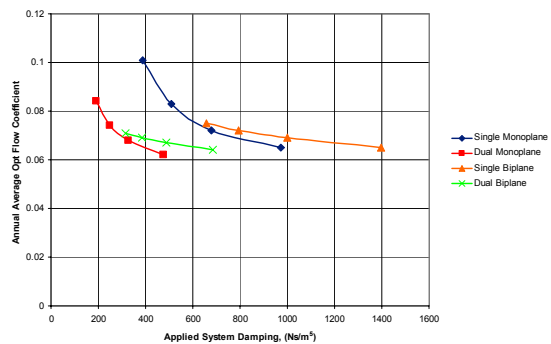


Figure 14: Annual Optimum Operating Flow Coefficient vs Applied System Damping

Time domain simulation models of varying degrees of complexity have also been developed over the years. They are used for studying control algorithms and how this affects the systems behaviour, refer to paper (10) for further details.

2 Structural Component Performance

Fatigue Analysis of Wells Turbine Blades

To calculate a fatigue life for the Wells turbine blades used in Wavegen's 18.5kW turbine, the material, loading and geometry were modelled. Previous fatigue estimations for LIMPET blades were reviewed and further developed for the 18.5kW turbine.

Modelling the S-N curve

To build a model of an S-N curve with limited test data, a linear relationship may be assumed between three points. The initial point is the material ultimate tensile stress, S_u . The next point is a stress value at $N=1 \times 10^3$ cycles. This value is $0.75 \times S_u$ for tension loads. Assuming S_u of the blades to be 290 MPa gives a value of 217.5 MPa.

The final point is the material's fatigue limit. Ferrous metals have a stress amplitude where the S-N curve becomes horizontal, stresses below this limit will not cause the material to fail under fatigue. Non-ferrous materials such as aluminum do not have such a characteristic limit and so a value, the endurance limit, is taken at a high number of cycles such as $N=5 \times 10^8$. The endurance limit of a test sample is then modified to relate it to a real life component using equation 1.

$$S_e = C_s \times C_r \times C_f \times C_1 \times C_t \times C_m \times S'_e / K_f \quad (\text{Eq. 1})$$

Variables are defined below:

Test Sample Endurance Limit, S'_e

CINDAS data supplied by Howden give the S-N curve for 5083 alloy exposed to air. The data gives a near linear relationship when plotted on a log-log scale and was extrapolated forward to $N=5 \times 10^8$ cycles, giving an endurance limit of $S'_e = 65.7 \text{ MPa}$

Size Factor, C_s

For the 18.5kW turbine the cross sectional area is 3818.34 mm^2 , giving a size factor of $C_s = 0.816$.

Reliability Factor, C_r

To allow for the statistical nature of fatigue, a reliability factor can be used to give a desired component reliability. A 99% reliability was selected, giving $C_r = 0.814$

Surface Finish Factor, C_f

The 18.5kW turbine blades have a machined finish which gives to a surface factor of $C_f = 0.85$.

Loading Factor, C_1

For the Wells turbine loading, take $C_1 = 0.85$

Temperature Factor, C_t

The turbine blades operate in a temperature of around 20°C so temperature effects can be ignored and $C_t = 1$.

Miscellaneous Factor, C_m

This parameter was used to account for various factors which were harder to quantify such as the effects of corrosion, surface coatings, etc. Corrosion combined with cyclic loading will lead to an accelerated failure and a lower than expected endurance limit due to the interaction of the corrosion and the loading.

Test sample data was supplied to Wavegen by Howden for the similar 5086 alloy exposed to air and salt water. For this data, the stress for failure after $N=5 \times 10^8$ cycles was found to be 7.4 MPa, compared to 114 MPa for the sample in air. The more corrosive atmosphere gives a value 6.5% of that in air. This was a rough estimation but is based on the only available data relating to the effects of corrosion fatigue. The miscellaneous factor, is thus $C_m = 0.065$

Fatigue Sensitivity, K_f

Fatigue sensitivity, K_f , relates the stress concentration factor to observed results in materials by using a notch sensitivity factor. For aluminum 5083-O, $K_f = 1.35$

Modified Endurance Limit

Combining all the above correction factors into equation 1 gives a modified endurance limit of:

$$S_e = 1.53 \text{ MPa}$$

Plotting the Results

Taking the y-intercept to be the ultimate tensile strength, S_u of the material (290 MPa) and plotting the two points calculated above, the modified S-N curve of the 18.5kW blade is shown in Fig.15.

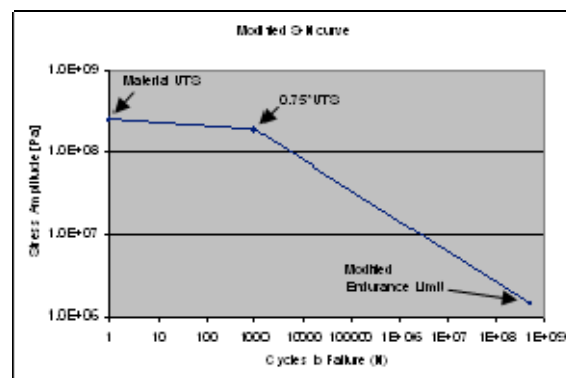


Figure 15: S-N curve for 18.5kW turbine blades

The equations for the two lines which make up the modified S-N curve are put into the Excel spreadsheets used for calculations and are used to calculate the number

of cycles to failure for each stress cycle, refer to (11) for further details.

Modelling the Loading

To model the loading, wavetank test data was used. The tank tests were conducted for 14 sea states representative of data measured by a waverider buoy off Mutriku. The data from the tank tests (a pressure trace of 8192 data points against time for each sea state) was then processed by a model to convert the pressure trace to a pressure across the blades and a revolution speed.

In addition to the loading on the blades during operation, there is a stress reversal every time the turbine is run up to speed and then stopped. On the main Limpet turbine this was observed to occur roughly 3 times a day. The small turbine (Mk I - IV) has been observed to run for weeks at a time in good conditions. As a conservative estimate, the number of start-stop cycles was modelled at one occurrence per day.

Modelling the Geometry

A finite element analysis was performed using ANSYS Workbench on a model of the turbine blades to find Von Mises stresses under two load conditions. The first load condition modelled the bending stresses created by a pressure drop (25KPa) across the blades, ref. Fig. 16. The loading created a tension stress on one side of the blade root and a compression stress on the other. The magnitude of the stresses at the blade root is proportional to the pressure so a stress factor for the pressure loading was found.

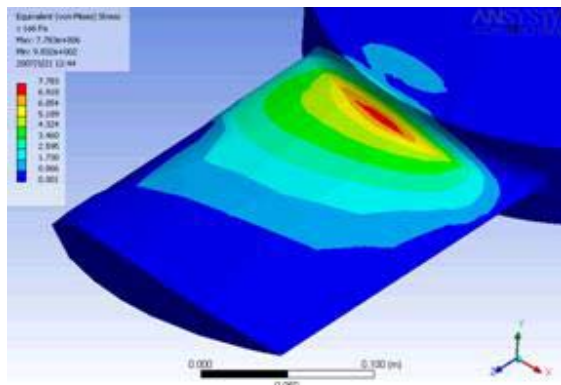


Figure 16: Von Mises stresses from 25kPa pressure

The second load condition was a rotational speed (4000 rpm, shown in Fig. 17). The stress value was taken at the position of maximum bending stress as well as the maximum stress for this load condition. The magnitude of the stresses at the blade root from this loading is proportional to the rotational speed squared and so a stress factor for rotational speed was found.

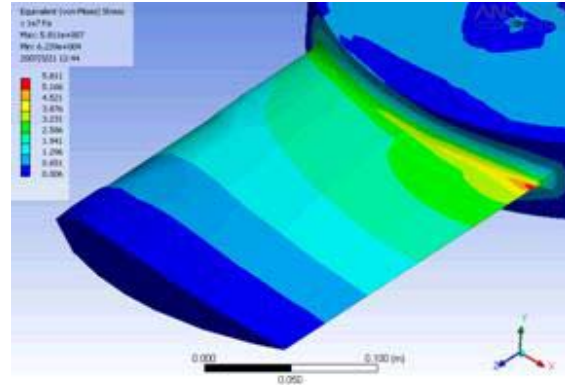


Figure 17: Von Mises stresses at 4000rpm rotation

Fatigue Analysis

The loading, geometry and material models were combined in an Excel workbook to create a fatigue life prediction. A macro was created which read in the loading history for each sea state (pressure and speed), analysed and recorded the data before moving onto the next sea state. The pressure and rotation were converted into Von Mises stresses using the stress factors found in the FE analysis. The stresses were then added together to give a total stress.

The macro then sorted through the data, picking out the turning points in the stress history to give a series of stress reversals. The stress history was then re-ordered to give the highest peak first, any data from before the highest peak was added to the end of the stress history. This was done to prepare the data for a rainflow cycle counting process. The stress history was then analysed using a rainflow method to give a series of mean stresses with alternating stress components. From this point, Goodman's rule (Equation 2) was applied to combine the two components into an equivalent stress.

$$S_e = \frac{S_A}{1 - \frac{S_M}{S_u}} \quad \text{Eq. 2}$$

For each stress reversal the equivalent stress was found and evaluated using the modified S-N curve calculated earlier to give the number of cycles to failure at that stress level. Miner's rule was then used to give a cumulative amount of damage done for each sea state. With the percentage applicability of each sea state known, the total annual contribution to fatigue from the wave loading was found. This fatigue damage was combined with the damage created from the start-stop cycles to give an overall fatigue life prediction of 44 years.

Bearing Life

To calculate bearing life for the proposed Mutriku turbines a model of the loading was required. To build the loading model, the pressure and speed history created after wavetank tests for each sea state was used. To convert the

alternating pressure load to an equivalent load, the alternating load was broken into discrete sections and number of revolutions at each load found. The overall maximum and minimum pressures were found and a histogram used to sort the data into pressure bins. Combining these histograms with sea state applicability, the overall percentage occurrence of each pressure bin can be found.

Each sea state has a mean speed associated with it so the number of revolutions in a year for each loading (U_i revolutions at load F_i) can be found and an equivalent load calculated. To account for a vertically mounted unit with the rotor weight supported axially, the rotating weight was subtracted from the alternating load before the absolute value was taken and put into equation 3 to find the equivalent axial load, F_a .

$$F_a = \sqrt[3]{\frac{F_1^3 U_1 + F_2^3 U_2 + \dots}{U}} \quad \text{Eq. 3}$$

For the Mutriku design the equivalent axial load was found to be 838 N. The radial load was calculated as an out of balance load which met balancing standard BS 6861 G6.3. Using the SKF bearing life methods⁽¹²⁾, calculation sheets were developed to allow quick estimations of bearing life to be made. Using these sheets a basic life of over 20 years was predicted with an 'SKF adjusted life' of over 50 years.

Wavegen Engineering Manual

Wavegen are developing an 'Engineering Manual' which will serve as a tool for product development, enabling rapid design work for project quotes. The work in this manual forms an important part of Wavegen's ISO 9001 accreditation. Historically, as most devices have been prototypes, Wells turbines have been a collection of bespoke sections, with the move towards designing turbines for commercial wave power plants, the engineering manual will provide standardisation of certain design processes.

The goals of the manual are as follows:

- To reduce the risk during layout, design, manufacturing and construction
- To reduce the time taken in design
- To lower the manufacturing costs through standardisation
- To create a uniform system for technical documentation and calculation

In constructing the manual, Wavegen's experience in Wells turbine design has been complimented by access to experts in axial fan and hydro power design through our parent company Voith Siemens Hydro.

The development of the 18.5kW turbine from Mk.I to Mk.IV has followed a development from prototype to commercial product, ref. Figs. 18 & 19. The manual will

provide a record of problems encountered and part failures and give details on how these were overcome and can be avoided in the future.



Figure 18: View from Attenuator Towards Rotors



Figure 19: View of Assembled Prototype Turbine

3 Acoustic Performance

Work carried out in conjunction with NEL^(13,14) has enabled the noise of the system to be measured and characterised at source, at near and far field conditions. The acoustic signature of the machine is complex due to the wide range of operational conditions. Classification and non -

dimensionalisation of the acoustic emissions enables comparisons to be made between the acoustic performance of different test turbine configurations in differing sea states. Predicting the sound power emissions of the source is required for environmental impact assessment of new developments and to impose constraints when producing viable design solutions which may be suitable for manufacture.

Long term acoustic measurements taken during operation of the small turbine have shown a strong correlation between the instantaneous sound emission and flow coefficient and turbine running speed, ref. Fig.19.

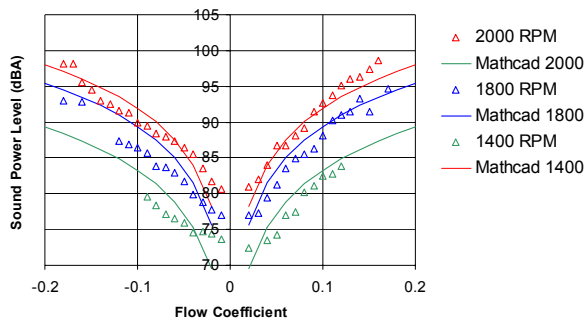


Figure 20: Variation of the Sound Power Level with Flow Coefficient and Turbine Speed

A mathematical model was constructed from fan based noise scaling laws⁽¹⁴⁾, to predict the instantaneous sound power (A weighted) for geometrically similar turbine designs with a given damping characteristic across the expected range of operating points. The turbine is modelled as a dipole source with noise emission being dependant on the Reynolds Number and Mach Number. Fig.19 shows the correlation between the predicted levels and site measurements for a small turbine installation.

In the low flow region of the wave cycle, around the air turning point, a better fit is found using a propeller scaling law, dependant only on the rotational speed and diameter of a low bladed system. Figs.20 - 22 shows the correlation between the measured and modelled values at low flows using this relationship. It should be noted that the increased noise shown on the measured data at high speeds is likely to be a result of increased turbulence in the air flow due to shock wave/ vortex boundary layer interactions and valve modulation.

It is stressed that the values of sound power levels (SWL) given in the figures should not be translated directly as if they were sound pressure levels (SPL) in the environment local to OWC plant. The figures take no account of the influence of control strategy on noise generation or of the effects of attenuators, shielding and distance on perceived noise. It is clear that adequate steps must be taken in all projects to ensure no environmental noise nuisance.

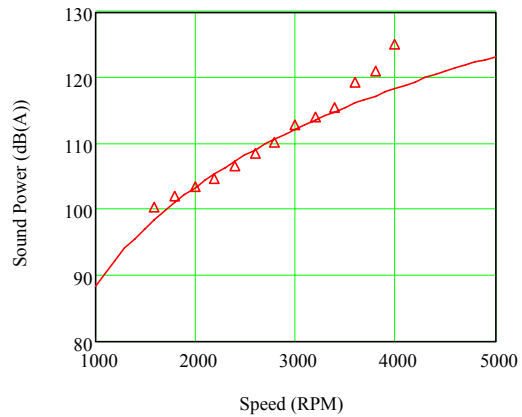


Figure 21: Variation of SWL with Turbine Speed

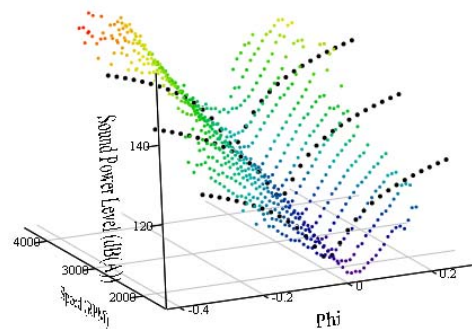


Figure 22: Correlation of SWL Acoustic Model with Site Measurements

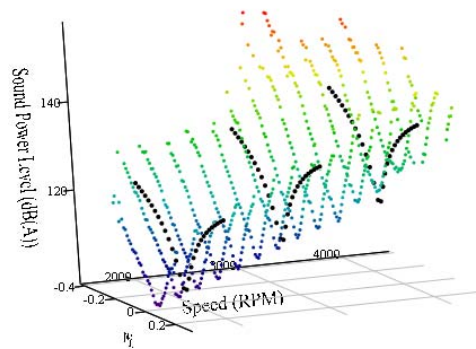


Figure 23: Correlation of SWL Acoustic Model with Site Measurements

Colours - Bin Averaged Experimental data
Black - Numerical data

As part of this process Wavegen has developed acoustic attenuation design methods in order to predict the sound emissions for proposed wave power schemes comprising multiple turbines.



Figure 24: Acoustic Test Facility at LIMPET

Construction of a plenum chamber (Fig.23) to enclose the small turbine on Islay and subsequent measurements taken inside and outside the plenum chamber have enabled the performance of a proposed attenuation scheme for a breakwater project (Mutriku) to be quantified and compared with modelled results. Additionally, frequency analysis of the turbine noise emission from measurements taken within the chamber has enabled the modelling of local noise propagation and selection of appropriate attenuation media in order to produce an acoustic design which will satisfy the local noise regulatory authorities.

Conclusions

(1) Parametric engineering design tools have been developed for optimisation of OWC power take-offs suitable for project use.

The main output of which is:

- a.) Performance predictions and optimum operating speeds.
- b.) Prediction of the sound power levels generated by the plant.
- c.) Noise attenuation design algorithms.
- d.) Fatigue life predictions of critical components.
- e.) Structural resonance checks via FEA analysis and measurement checks.
- d.) Bearing life prediction.
- e.) Cost estimation of plant.

References

- [1] A. F. de O. Falcão and R.J.A. Rodrigues. Stochastic Modelling of OWC Wave Power Plant Performance. *Applied Ocean Research* 24, pp59-71, 2002.
- [2] A. F. de O. Falcão. Control on an Oscillating Water Column Wave Power Plant for Maximum Energy Production. *Applied Ocean Research* 24, pp73-82, 2002.
- [3] A. F. de O. Falcão. Maximum Energy Production and Maximum Profit as Alternative Criteria for Wave Energy Power Equipment Optimization. In *Proc. 5th European Wave Energy Conference*, Cork, Ireland, September 2003.
- [4] L.M.C. Gato, P.A.P. Justino and A. F. de O. Falcão. Optimisation of Power Take-off Equipment for an Oscillating Water Column Wave Energy Plant. In *Proc. 6th European Wave and Tidal Energy Conference*, Glasgow, 2005.
- [5] R. Curran and L.M.C. Gato. The Energy Conversion Performance of Several Types of Wells Turbine Designs. *Proc. Instn. Mech. Engrs.* Vol. 211 Part A, 1996.
- [6] L.M.C. Gato and A. F. de O. Falcão. On the Theory of the Wells Turbine, *Transactions of the ASME*, 628, Vol. 106, July 1984.
- [7] L.M.C. Gato and A. F. de O. Falcão. Aerodynamics of the Wells Turbine, *Int. J. Mech. Sci.*, Vol. 30, No.6, pp383-395, 1988.
- [8] C.P. Tan. Predictions and Experimental Investigations on the Performance of Wells Air Turbine. PhD Thesis, Aeronautical Engineering Dept., Queen's University of Belfast, August 1983.
- [9] H.A. Heikal, A.A. Hafiz, N.N. Bayomi and M.H. Ahmed. Theoretical and Experimental Investigation on the Wells Turbine Performance, pp213 - 233.
- [10] R.G.H. Arlitt, W.K. Tease, R. Starzmann and J. Lees. Dynamic System Modelling of an Oscillating Water Column Wave Power Plant based on Characteristic Curves obtained by Computational Fluid Dynamics to Enhance Engineering Reliability. In *Proc. 7th European Wave and Tidal Energy Conference*, Porto, 2007.
- [11] H.A. Rothbart. *Mechanical Design Handbook*. McGraw-Hill, 1996.
- [12] SKF, General Catalogue 5000E, June 2003.
- [13] R. Whitson, 'Airborne, Waterborne and Rockborne Noise Measurement Issues on a Shoreline Based Wave Energy Device', NEL report No. 2005/244, March 2006.
- [14] W.K. Tease, J. Lees and R. Whitson. Preliminary Noise Measurements Taken on an Oscillating Water Column Wave Power Device. Noise and Vibration in Marine Applications Seminar 27 September 2006.

